Analytical Study of Boosted Lubrication for Synovial Ankle Joint

Dr. Kadhum Audaa Jehhef
kadhum.audaa@yahoo.com
Middle Technical University-Institute of Technology
Department of Machine and Equipment - Baghdad, Iraq
Dr. Safaa A. Ghadhban
safaaabid@yahoo.com
Middle Technical University - Electrical Engineering Technical College - Department of Electrical Power Engineering Techniques - Baghdad, Iraq

Abstract

The modeling of the lubrication of human ankle joint has been considered in this present research. Many parameters were carried out such as joint geometry parameters as (minimum film thickness h, radial clearance c, Eccentricity e), lubricant parameters as (synovial fluid viscusity μ, couple stress property η) and cartilage matrix parameters as (Ratio of microstructure size to pore β, Permeability of the cartilage ϕ, Porous layer thickness H). The effects of these parameters on the synovial fluid velocity, pressure in the porous region, load carrying capacity per unit length of the bearing and the coefficient of friction were investigated. The model starts from the theory of boosted lubrication for the human articular joints lubrication and takes into account the fluid transport across the articular cartilage using Reynolds equation and modified Darcy's equation. The results show that the pressure

increased with increasing the couple stress length and the eccentricity ratio parameters. The synovial velocity profile was changing from Newtonian at (l=0.0) to non-Newtonian profile as increasing the couple stress length. Finally the coefficient of friction increases with decreasing the eccentricity ratio and with increasing the joint radial clearance.*

Keywords: ankle joints, boosted lubrication, synovial joints lubrication.

Nomenclatures

A tibial length
AC articular cartilage
c radial clearance
Cf coefficient of friction
e eccentricity parameter, mm
fr synovial fluid film force
H porous layer thickness
h synovial film thickness
h* dimensionless minimum film thickness
H_o minimum film thickness, ho/R
h_{tal} talus cartilage thickness, mm
h_{tib} tibia cartilage thickness, mm
l couple stress parameter
L talus length (bearing length), mm
L* dimensionless bearing length
l* dimensionless couple stress parameter
p pressure in the film region
p* dimensionless pressure
R_{tal} radius of journal (radius of talus bone average), mm
R_{tib} radius of bearing (radius of tibia bone average), mm
t time.
u,v components of fluid velocity in x, y directions respectively
W load carrying capacity
x,y dimession axis, m

Greek symbols:

α percolation parameter.
ε eccentricity ratio (e/c)
ε eccentricity ratio
η material constant accounting for couple stress
θ circumferential coordinate
μ viscosity of synovial fluid, Pa.s
ρ synovial fluid density, kg/m^3
ϕ permeability of the cartilage matrix, m^2

1. Introduction

The increasing importance of human joints study as complex mechanical systems involves medical data processing, system fluid lubrication film, dynamic modeling and the establishing of reliable boundary conditions. Understanding the dynamical behavior of joints is crucial to face prosthesis design and the associated research. The squeeze film lubrication phenomenon is observed in several bio-applications such as human joints hip, knee and ankle (Lin, et. al. 2004) [1]. A simple analysis of squeeze films between compliant surfaces and application of analysis experimentally to synovial joint strongly (Fein, 1967) [2] presented analysis for the minimum film thickness in the hip, knee, and ankle joints. They pointed out that for high loads with short duration the squeeze film mechanism looks very promising. (Edwards, 1967) [3] discussed the structure of articular cartilage and he demonstrated that its physical behavior is of particular importance in joint lubrication. The first experimental and theoretical study on the squeeze film phenomenon in the ankle joint was presented by (Medley, 1981) [4]. Who investigated the geometry, friction and lubrication of normal human ankle joints. He developed theoretical models to estimate the cyclic variation in elastohydrodynamic film thickness and coefficient of friction for the ankle during walking. And he used theoretical minimum film thicknesses of about 1 μm. His study indicated that full fluid film lubrication cannot be sustained. (Medley, et. al., 1983) [5] they studied the Human ankle joint specimens and the dimensions required for lubrication analysis. The radii of curvature of the tibial surfaces were slightly larger than

those of the corresponding regions of the talar surfaces. (Medley, et. al., 1984) [6] proposed an equivalent bearing to represent the normal human ankle joint. They developed theoretical models to estimate the cyclic variation in lubricant film thickness and coefficient of friction during repetitive activities such as walking. For the conditions representing the walking cycle, film thicknesses of about 0.7 μm were calculated. The mixture model of synovial fluid filtration by cartilage in the human ankle joint during walking is presented for steady sliding studied by (Miroslav, 1999) [7]. He assumed that the synovial fluid is Newtonian and physiologic parameters of the ankle joint during walking, a continuous synovial fluid film about 1μm thick is maintained under steady entraining motion according to the classical model without the fluid transport across the articular surface.

The simple homogeneous model for articular cartilage models the case of early osteoarthritis presented by (Hlavacek, 2000) [8] for a squeeze film lubrication model of the human ankle joint in standing that takes into account the fluid transport across the articular surface. His calculations indicated for this case that in normal approach motion the lubricating fluid film is quickly depleted and turned into a synovial gel film that is supposed to serve as a boundary lubricant in sliding motion. (Ruggiero, 2010) [9] presented an analytical approximate squeeze-film lubrication model of the human ankle joint when the load carrying due to the squeeze motion. The model starts from the theory of boosted lubrication for the human articular joints lubrication and takes into account the fluid transport across the articular cartilage using Darcy's equation. (Miroslav, 2009) [10] studied the lubrication of the human ankle joint in steady running, synovial fluid is considered Newtonian, and biphasic mixture model is considered for articular cartilage. This model indicates that during running, similarly to walking, the joint operates in a mixed lubrication mode (a combination of the boundary and fluid film lubrication), but as compared to walking, with a major emphasis on the fluid film mode. (Alessandro, et. al., 2010) [11] used an analytical approximate squeeze-film lubrication model of the human ankle joint for a quick assessment of the synovial pressure field and the

load carrying due to the squeeze motion, considering both normal and pathological behavior was obtained. (Yousif and Al-allaq, 2013) [12] derived Reynolds equation with the synovial fluid as a couple stress fluid and transport across the articular cartilage matrix using a modified Darcy's equation. They show, in the presence of porous articular cartilage the pressure distribution, load carrying capacity, synovial film thickness with time of approach increased and a reduction of coefficient of friction. Finally (Amato, et. al., 2015) [13] used proper medical image segmentation, bone surfaces are 2D modeled as constant curvature surfaces (circles) under different criteria. This study aims to investigate all allowed parameters and its effects on the lubrication ankle joint using the analytical and numerical solution.

2. Mathematical model

2.1 Surface Geometry of the Ankle Joint

The study of the human ankle joint in particular must include some knowledge of the local anatomy. The bones in the vicinity of the ankle joint are shown in Fig.1. The ankle joint referred to as the talocrural joint, permits rotation of the foot in a posterior-anterior plane of vertical orientation. The raising of the toes and lowering of the heel involves flexion. The side-to-side motion of the foot, or rotation in a medial-lateral plane of horizontal orientation involves the subtalar joint between the talus, navicular and calcaneus bones. The ankle joint itself is composed of three pairs of articulating surfaces between (Medley, 1981) [4]: Medial malleolus and talus, Tibia and talus and Lateral malleolus and talus.

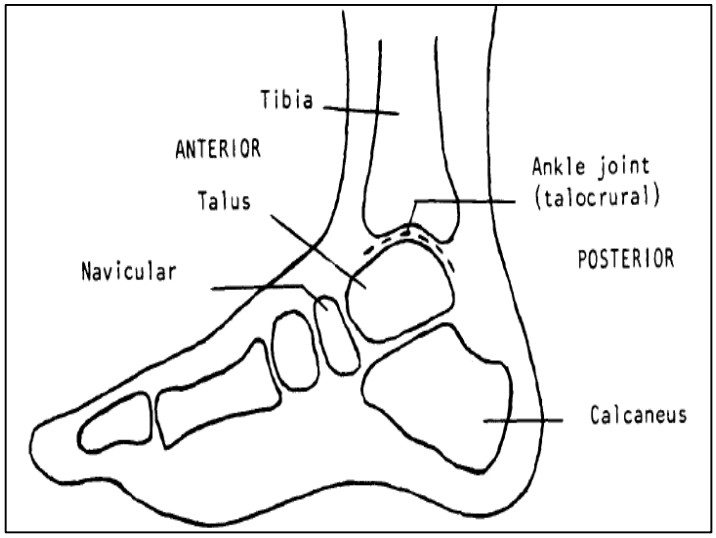

(a)

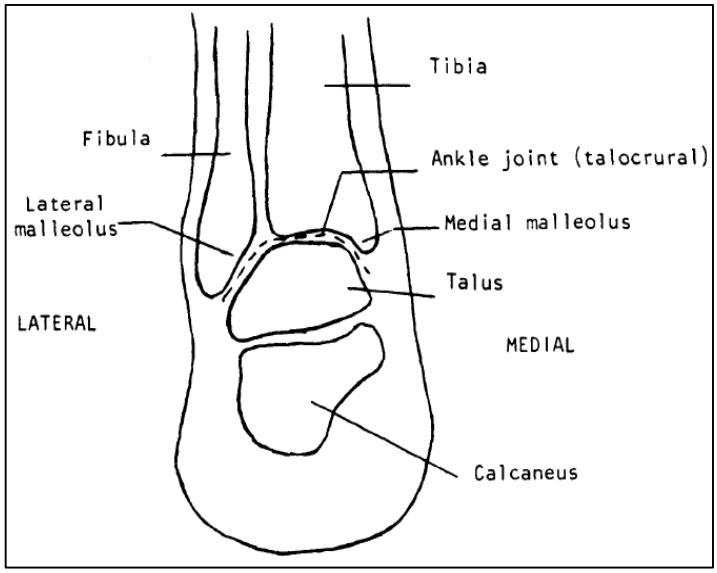

(b)

Fig.1: a) Sagittal section; b) Frontal of the foot showing bone structure Medley, (1981) [4].

2.2 Fluid Film Mechanism

When a fluid lubricant is present in a bearing, films can be generated by the motion of converging-diverging surfaces. If the

bearing surfaces remain rigid, the process by which fluid films are entrained I known as hydrodynamic lubrication as shown in Fig.2a. However, when the film pressures are large enough to deform the surfaces the region of contact is increased. This reduces the film pressures required to balance the applied load. This mechanism is called elastohydrodynamic lubrication and is depicted in Fig.2b. The possibility of elastohydrodynamic lubrication of this type occurring in synovial joints has also been examined (Dowson, 1980) [14].

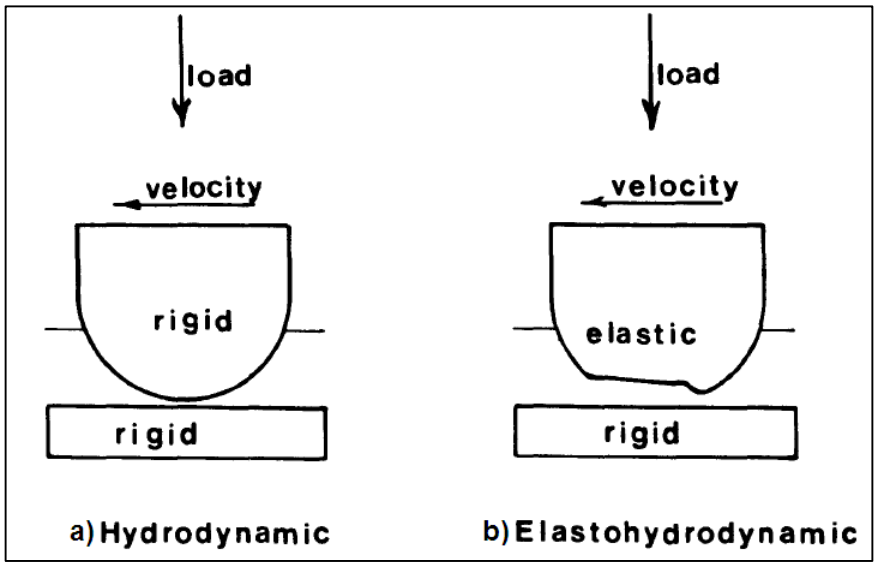

Fig.2: Hydrodynamic and elastohydrodynamic lubrication.

The follwing informatiom Table.1 was obtianed according to the geometry information from proper medical image segmentation, bone surfaces (tibial and talar bone surfaces) are 2D modeled as constant curvature surfaces (circles).

Table.1: Anatomy measured parameters involved by (Amato. et. al., 2015) [13].

Symble	Defination	Value	Unit
h	minimum film thickness	7×10^{-4}	mm
R_{tib}	radius of bearing (radius of tibia bone average)	23. 5	mm
R_{tal}	radius of journal (radius of talus bone average)	22.3	mm
L	Talus length (bearing length)	35	mm
e	Eccentricity parameter	1.234	mm
C	radial clearance	1.2×10^{-2} - 1.2×10^{-5}	m
h_{tib}	Tibia cartilage thickness	1.4	mm
h_{tal}	Talus cartilage thickness	1.4	mm
ε	Eccentricity ratio	0.1-0.6	-
h*	Dimensionless minimum film thickness	0.9655	-
l*	Dimensionless couple stress length	0.1-0.5	-
ϕ	Permeability of the cartilage matrix	10^{-7}-10^{-8}	m^2
μ	Viscosity of synovial fluid	0.01-0.03	Pa. s

2.3 Mathematical modeling

The human ankle joint can be considered as cylindrical. The motion is allowed only in the sagittal plane; the coupling model is assumed by two infinite rigid circular cylinders (subchondral bone) in the internal contact (a cylinder encased in a cylindrical cavity), covered with thin layer (articular cartilage) of uniform thickness; the lower (talar) articular surface is supposed stationary while the upper (tibial) surface is assumed to have pure squeeze motion; the lubricating gap is assumed to be filled with a SF film. Fig.3 show the model and the coordinates x and y used for the description of the fluid film pressure. Walicki, 2000[15]

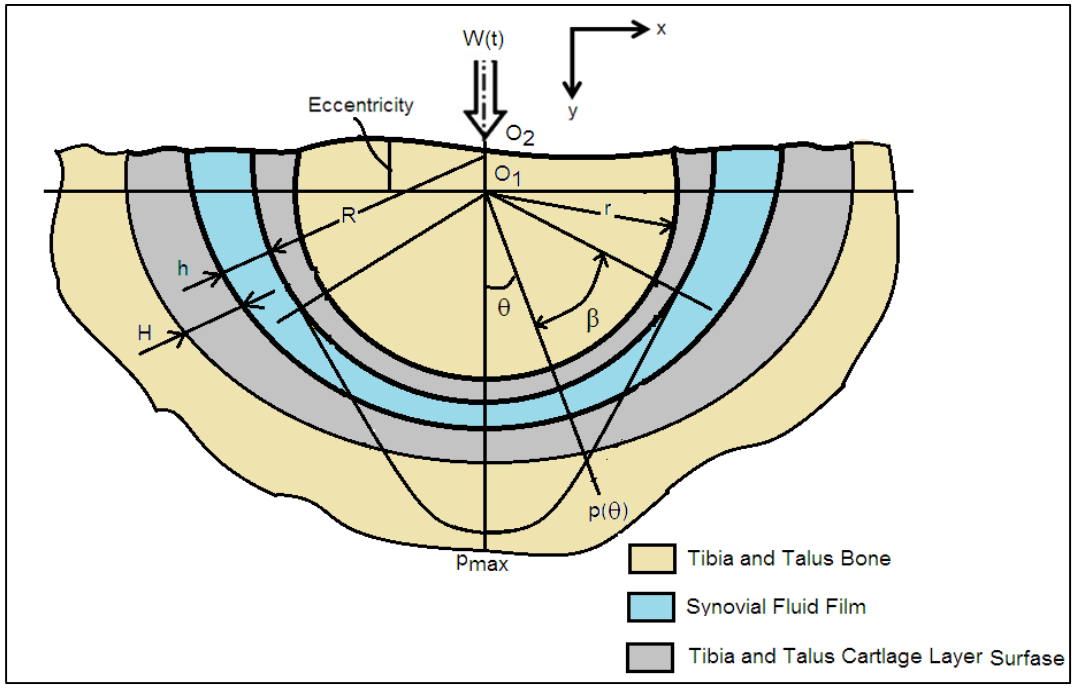

Fig.3: Theoretically possible configuration of the articular surfaces in the sagittal section of a loaded human ankle joint.

The movement occurs in the x-y plane, thus, articular surfaces move along y with a vertical non-stationary load W(t). The surface with its center at θ=0 is bounded with the edges at θ=±β in which the synovial pressure is assumed to be equal to zero. Only the symmetric case is considered in this paper allowing the obtained analytical results the generalization to the other non-symmetrical configurations. The thickness of the gap of two infinite circular cylinders can be written as:

$$h(x,t) = \check{h}(t) - 2\hat{h}$$

where $\check{h}(t)$ is the SF film thickness including cartilage surfaces and $\hat{h}$ the thickness of the cartilage surfaces. The joint cavity is filled with synovial fluid. Its viscosity depends upon the content and molecular size of the hyaluronic acid component (Walicki, 2000) [15]. Couple stresses are found to appear in noticeable magnitude in liquids with very large molecules. The long chain polysaccharide hyaluronic acid molecules present in the synovial fluid gives the

motivation for assuming the synovial fluid as a Stokes couple-stress fluid (Bujurke, et.at, 1990) [16]. It is characterized by two material constants (μ and η), whereas only one parameter μ appears in the model of viscous fluid when the body forces and body movements are absent. The equation of motion for incompressible couple-stress fluid derived by Stokes, using the usual notation is: The basic field equations of the micropolar fluid were developed by (Eringen, 1964) [17]. The basic equations for the flow of micro polar fluid in the film region in vectorial form are:

$$\nabla V = 0 \quad (1)$$

in vector form it given by:

$$\rho \frac{DV}{\partial t} = -\nabla p + \mu \nabla^2 \vec{V} - \eta \nabla^4 \vec{V}$$

(2)

or in differential form it given by:

$$\rho \left[u \frac{\partial u}{\partial x} + w \frac{\partial u}{\partial y} \right] = -\frac{\partial p}{\partial x} + \mu \frac{\partial^2 u}{\partial y^2} - \eta \frac{\partial^4 u}{\partial y^4} \quad (3)$$

μ has the dimensions of viscosity, whereas η has the dimensions of momentum. The ratio (η/μ) is of dimensional square length and hence characterizes the chain length (Alessandro, et.al., 2013) [18].

$$l = \sqrt{\frac{\eta}{\mu}} \quad (4)$$

Under the usual assumptions of fluid film lubrication applicable to thin films, the equation of motion of an incompressible couple stress fluid within the film region (Bujurke, et. al., 2006)[19], then equation (3) becomes:

$$\frac{\partial p}{\partial x} = \mu \frac{\partial^2 u}{\partial y^2} - \eta \frac{\partial^4 u}{\partial y^4} \quad (5)$$

$$\frac{\partial p}{\partial y} = 0$$

(6)

$$\frac{\partial p}{\partial z} = \mu \frac{\partial^2 w}{\partial y^2} - \eta \frac{\partial^4 w}{\partial y^4} \quad (7)$$

The governing steady-state laminar equation of motion the fluid film region in Cartesian coordinates is the continuity equation:

$$\frac{\partial u}{\partial x} + \frac{\partial v}{\partial y} = 0 \quad (8)$$

The boundary conditions, for pure squeeze film motion under the hypothesis of no sleep condition at the interfaces are:

$$u(x,-h,z) = u(x,0,z) = \frac{\partial^2 u}{\partial y^2} \quad (9)$$

The flow of couple stress fluid in a porous matrix is governed by the modified Darcy law, which accounts for the polar effects (Naduvinamani et. al., 2005) [20].

$$\vec{q} = \frac{-\emptyset}{\mu(1-\beta)} \nabla p \quad (10)$$

where

$\overrightarrow{q^*} = (u^*, v^*)$

ϕ is the permeability of the porous matrix, the dimensionless parameter β represents the ratio of microstructure size to the pore size and is:

$\beta = (\eta/\mu)/\emptyset = (l^2/\emptyset)$

When the microstructure size is very small compared to the pore size, i.e. ($\beta << 1$), the hyaluronic acid molecules percolate into the porous matrix. In the limit as ($\beta > 0$) the joint conditions tend to the case of the Newtonian flow in the porous matrix. Integrating Eqs.(5) and(7) by applying the related boundary conditions:

$$u(y) = \frac{1}{2\mu}\frac{\partial p}{\partial x}\left\{ y(y-h) + 2l^2\left[1 - \frac{cosh\left(\frac{2y-h}{2l}\right)}{cosh\left(\frac{h}{2l}\right)}\right]\right\} \quad (11)$$

The relevant boundary conditions for the velocity components are:

i. At the porous journal surface y = 0:

$$u = 0, \quad \frac{\partial^2 u}{\partial y^2} = 0 \quad and \quad V = v^* \quad (12)$$

ii. At the boundary surface y = h:

$$u = 0, \quad \frac{\partial^2 u}{\partial y^2} = 0 \quad and \quad V = -v_\theta \quad (13)$$

Squeeze film pressure of the partial porous journal bearing

By using the Squeeze film pressure of the partial porous journal bearing representing the ankle joint Equation of velocity with angle:

$$v_\theta = -\frac{\mathrm{dh}}{dt} = C\frac{\mathrm{d}\varepsilon}{dt}cos(\theta) \quad (14)$$

The equation of film thickness in journal bearing (Bujurke, et. al., 2006) [19]:

$$h = C - e\,cos(\theta) = C[1 - \varepsilon cos(\theta)] \quad (15)$$

Introducing the non-dimensional quantities in the governing equations for pressure is of importance for both theoretical and computational purposes. It is also of importance of various terms in the lubrication system (Alessandro et. al., 2013) [18].

$$R^* = \frac{R}{C}\ , \quad \Psi^* = \frac{\emptyset H}{C^3}\ , \quad h^* = \frac{h}{C} = 1 - \varepsilon\cos(\theta)\ , \quad p^* = \frac{pC^2}{\mu R^2\left(\frac{d\varepsilon}{dt}\right)}$$

$$\theta^* = \frac{X}{R}\ , \quad l^* = \frac{l}{C}\ , \quad \emptyset^* = \frac{\emptyset}{C^2}\ , \quad \varepsilon = \frac{e}{C}, \quad H^* = \frac{H}{C} \quad (16)$$

Derivation the modified Reynolds equation

Integration of continuity equation (8) to obtain:

$$\int_0^h \frac{\partial v}{\partial y}dy = -\int_0^h \frac{\partial u}{\partial x}dy \quad (17)$$

Apply the boundary condition of equations (11), (12) and (13) to equations (14) to get:

$$-v_\theta - \frac{\emptyset Ho}{\mu(1-\beta)}\frac{\partial^2 p}{\partial x^2} = -\frac{\partial}{\partial x}\int_0^h u\ dy \quad (18)$$

Using equation (16) and performing the integration:

$$\frac{\partial}{\partial x}\left\{\left[f(h,l) + \frac{12\emptyset Ho}{(1-\beta)}\right]\frac{\partial p}{\partial x}\right\} = -12\frac{\partial}{\partial x}v_\theta\mu \quad (19)$$

Apply equation (16) in equation (19) to obtain the final form of dimensionless modified Reynolds equation as:

$$\frac{\partial}{\partial \theta}\left\{\left[f(h^*,l^*) + \frac{12\emptyset^* H^*}{(1-\beta)}\right]\frac{\partial p^*}{\partial \theta}\right\} = -12\cos(\theta) \quad (20)$$

Where f (h*,*l**) is represented by:

$$f(h^*,l^*) = h^{*3} - 12l^{*2}h^* + 24l^{*3}\tanh\left(\frac{h^*}{2l^*}\right) \quad (21)$$

The boundary conditions for the fluid film pressure are:

$$p^* = 0 \quad at \quad \theta = \pm\frac{\pi}{2} \tag{22}$$

$$\frac{dp^*}{d\theta} = 0 \quad at \quad \theta = 0 \tag{23}$$

Integrating equation (21) with boundary conditions (22), (23) and inserting the two limits (θ, -π/2) to obtain final form of pressure distribution:

$$p^*(\theta) = \frac{-3(\pi^2 - 4\theta^2)}{2\left[(-1+\varepsilon)^3 - 12(-1+\varepsilon)l^2 - \left(\frac{12\emptyset^* H^*}{(1-\beta)}\right) - 24l^3 tanh\left(\frac{1-\varepsilon}{2l}\right)\right]} \tag{24}$$

Load carrying capacity of the porous partial journal bearing

Load carrying capacity of the porous partial journal bearing representing ankle joint. The load carrying capacity of the porous bearing in a squeeze action is obtained by integrating the film pressure equation acting on the surface of the journal shaft. The load carrying capacity is there given by:

$$W = \int_{-\frac{\pi}{2}}^{\frac{\pi}{2}} p(\theta).R.\cos(\theta) \tag{25}$$

Where (W) represents the load carrying capacity per unit length of the porous bearing generated by the squeeze film pressure. Let the dimensionless load carrying capacity be [Lin, 1997] [21] by:

$$W^* = \frac{WC^2}{\mu R^3\left(\frac{d\varepsilon}{dt}\right)}$$

$$W^* = \int_{-\frac{\pi}{2}}^{\frac{\pi}{2}} P^*(\theta).\cos(\theta).\mathrm{d}\theta \tag{26}$$

All mathematical analyses and output resulting curves were carried out by "MATLAB". This is a computational software program used in scientific, engineering, and mathematical fields and other areas of technical computing. The equation (26) becomes:

$$w^*(t) = \frac{-\pi^3(1280 - 32\pi^2 + \pi^4)}{1280\left[(-1+\varepsilon)^3 - 12(-1+\varepsilon)l^2 - \left(\frac{12\emptyset^* H^*}{(1-\beta)}\right) - 24l^3 tanh\left(\frac{1-\varepsilon}{2l}\right)\right]} \tag{27}$$

Squeeze Time-film thickness relationship

The most important characteristics of the squeeze film bearings is the squeeze film time, i. e., the time required for reducing the initial film thickness (h*) to (ho*) (minimum film thickness). The response time of the squeeze film is one of the significant factors for the understanding of biological bearings. The response time is the time that will elapse for a squeeze film to be reduced to some minimum permissible level. The film thickness at any time (t) can be obtained by integration equation (27) for the given load [**Sinha et. al. 1982] [22]:**

$$t^* = \int_h^1 W^* \mathrm{d}\varepsilon \qquad (28)$$

Coefficient of friction

The friction force can be obtained by integrating the shear stress around the journal surface, as follows [Mokhiamer, et al. 1999] [23].

$$\tau = \mu \left(\frac{\partial u}{\partial y}\right)_{y=h} - \eta \left(\frac{\partial^3 u}{\partial y^3}\right)_{y=h} \qquad (29)$$

The coefficient of friction can be calculated from the relation:

$$C_f = \frac{F^*}{W^*} \qquad (30)$$

Substituting for (F*) and (W*) from equation (27) and equation (30) respectively to get final equation of Coefficient of friction:

$$C_f = \frac{1280\left[(-1+\varepsilon)^3 - 12(-1+\varepsilon)l^2 - \left(\frac{12\emptyset^* H^*}{(1-\beta)}\right) - 24l^3 tanh\left(\frac{1-\varepsilon}{2l}\right)\right]}{-\pi^3(1280 - 32\pi^2 + \pi^4)}$$

$$\left[\frac{1}{1-\varepsilon} - \frac{\varepsilon}{6(-1+\varepsilon)^3} - \frac{3}{(-1+\varepsilon)^3 - 12(-1+\varepsilon)l^2 - \left(\frac{12\emptyset^* H^*}{(1-\beta)}\right) - 24l^3 tanh\left(\frac{1-\varepsilon}{2l}\right)}\right] \qquad (31)$$

$$\frac{3\varepsilon}{(-1+\varepsilon)^3 - 12(-1+\varepsilon)l^2 - \left(\frac{12\emptyset^* H^*}{(1-\beta)}\right) - 24l^3 tanh\left(\frac{1-\varepsilon}{2l}\right)}\Bigg]$$

To solve the above equations using the MATLAB program flow chart presented in Fig.4 below:

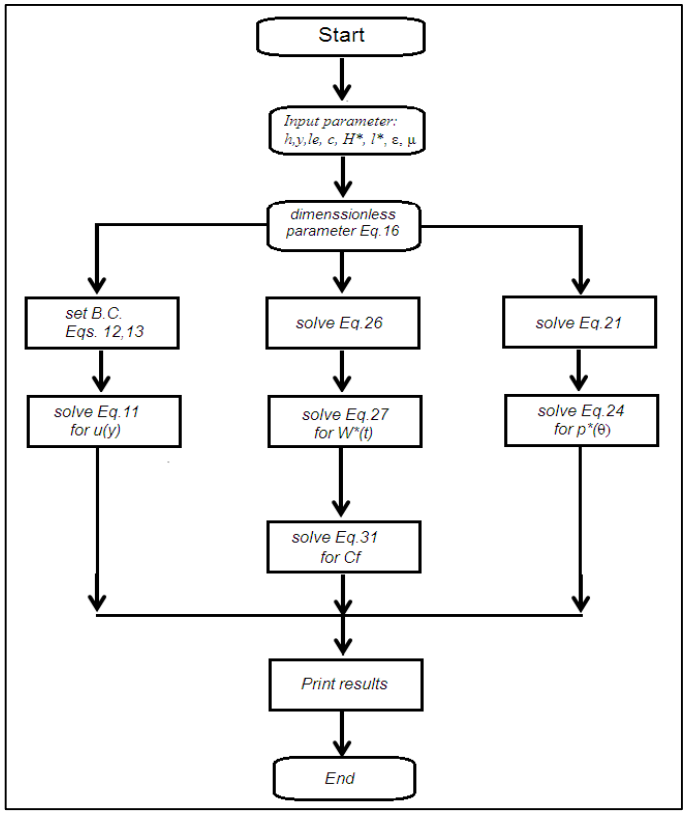

Fig.4: MATLAB program flow chart for present work calculation.

3. Results and discussion

In this paper the 2D metrological characterization in the sagittal plane of the articular surfaces in the lubricated contact of the human ankle joint has been studied theoretically. The behavior of the synovial fluid has been assumed to be isothermal, shear thinning and non- Newtonian couple stress fluid. The model of ankle joint has been taken geometrically and kinematically as a partial porous journal bearing under the action of hydrodynamic squeeze film lubrication. A modified Reynolds equation has been derived with the synovial fluid as a couple stress fluid and transport across the articular cartilage matrix using a modified Darcy's equation. As showed in Fig.5 that the dimensionless pressure (p*) increased with increasing the different dimensionless couple stress length

parameters of the synovial fluid. The bearing material consists of a thin layer of cartilage, which is a viscoelastic material having a high porosity and low permeability. Also, Fig.6 showed that the dimensionless pressure (p*) increased with decreasing synovial fluid permeability value of the cartilage matrix permeability (Ø). When cartilage deforms under load the permeability of the proteoglycan gel allows the weakly bound interstitial fluid to be mechanically squeezed out to join the free interstitial fluid. The free interstitial fluid can move within the cartilage, away from the loaded regions, and across the cartilage surface into the synovial fluid. This fluid motion is impeded, and thus deformation resisted, by the small size of the pores within the proteoglycan gel and between the collagen fibers. Moreover the dimensionless pressure (p*) increased with increasing the dimensionless eccentricity ratio (ε*) as plotted in Fig.7. In this study having an increased effect of dimensionless couple stress length parameter (l*) on the synovial fluid film axial velocity (u) velocity patterns changed as plotted in Fig.8, it showed that the increasing couple stress (*l**) from Newtonian limit at (*l**=0) to higher value show that the velocity had been become more and more flatter along the longitude direction line due to the non-Newtonian effects were appeared. But the effect of synovial film thickness (h*) on the synovial fluid film axial velocity (u) was presented in Fig.9 it showed that for each value of film thickness (h) there is a profile of synovial fluid film axial velocity (u) and give the maximum velocity but the maximum velocity was found at (h=2.5). Fig.10 presents the effect of synovial fluid (μ) on the synovial fluid film axial velocity showed that the maximum synovial fluid film axial velocity was decreased with increasing the viscosity of synovial fluid (μ). When a very considerable increase in the bulk viscosity of the lubricant was introduced into the calculations film thicknesses of about 18 μm and coefficients of friction up to 0.01 were estimated. This value for film thickness was sufficient to separate the surface asperities of healthy articular cartilage. Viscosity decreases as shear rate increases and eventually approaches a constant value that is somewhat larger than that of water. The effect dimensionless couple stress length parameters (l*), permeability value of the

cartilage matrix (Ø), dimensionless eccentricity (ε*) and porous layer thickness (H) on the dimensionless load capacity illustrated in Fig.11 to 14 showed that the dimensionless load increased with increasing the dimensionless eccentricity ratio (ε*) and decreasing with increasing the couple stress length parameters (l*) as illustrated in Fig.11. In Fig.12 can be show that the permeability (Ø) has no effect on dimensionless load. The effect of permeability value of the cartilage matrix (Ø) on the variation of dimensionless load capacity (W*) with different value porous layer thickness (H) at (ε = 0.2), (β=0.3), (h*=0.3), (l*=0.3) is plotted in Fig.14, it showed that the dimensionless load (W*) decreasing with increasing the permeability, however, one can see that the dimensionless load increased with decreasing porous layer thickness (H). The decreasing of the dimensionless synovial film thickness (h*) cause to increasing the dimensionless response time (t*) as shown in Fig.15 at constant values of permeability value of the cartilage matrix (Ø) by a constant profile. Also, the decreasing of porous layer thickness (H) will cause to increase the dimensionless response time but with a linear relation as a function to cartilage matrix (Ø) as plotted in Fig.16. The coefficient of friction (Cf) of the synovial ankle human joint was presented in Fig.17 and Fig.18. It drawing with a relation with the dimensionless couple stress length parameter (l*) and the radial clearance (c), the figures show that the coefficient of friction (C_f) will decrease with the dimensionless couple stress length parameter (l*) and increasing with the radial clearance (c) at constant dimensionless eccentricity ratio (ε*) and cartilage matrix (Ø). Finally to validate the present analytical results with previous works, using the results of dimensionless pressure (p*) with tilt angle (θ) with result of (Amato, et. al., 2015) [13] at (ε = 0. 2), (β=0.3), (h*=0.3), (l*=0.3) plotted in Fig.19 show good agreement in this range.

4. Conclusions

The theory of boosted lubrication for the human articular ankle joints lubrication was considred where the fluid transport across the articular cartilage using Reynolds equation and modified Darcy's equation. The problem of ankle joint lubrication has been solved

numerically. The theoritecal results show that the dimensionless pressure increased with increasing the dimensionless couple stress length (l*) and dimensionless eccentricity ratio (ε*) parameters, the synovial velocity profile was changing from Newtonian at (l*=0.0) to non-Newtonian profile as increasing the dimensionless couple stress length. The coefficient of friction (C_f) decreasing with increased the eccentricity ratio (ε*) and increasing with increasing the radial clearance (c). Finally the coefficient of friction (C_f) was perform littel effected by the cartilage matrix (Ø)

References

[1] Lin J. R., Liao W. H., Hung C. R., "The effects of couple stresses in the squeeze film characteristics between a cylinder and a plane surface", Journal of Marine Science and Technology, Vol. 12, No. 2, 2004, pp. 119-123.

[2] Fein, R. S., "A Synovial Joints Squeeze-Film Lubricated", Lubrication and Wear in Living and Artificial Human Joints, Proc.I. Mech. Engs., 181, 3J, 1967.

[3] Edwards, J., "Physical Characteristics of Articular Cartilage", Lubrication and Wear in Living and Artificial Human Joints, Proc., I., Mech., Engs., 181, 3J, 1967.

[4] Medley, J. B., (1981) "The Lubrication of Normal Human Ankle Joins" A PhD thesis, Department of Mechanical Engineering The University of Leeds, England November 1981.

[5] Medley J. B., Dowson D., Wright V., (1983), "Surface geometry of the human ankle joint", Medical Engineering & Physics limited, Vol. 12. No. 1, 1983, pp. 35–41.

[6] Medley J. B., Dowson D., Wright V., (1984),"Transient elasto-hydrodynamic lubrication models for the human ankle joint", Medical Engineering & Physics limited Vol. 13 No. 3, 1984, pp. 137-151.

[7] Miroslav H. "Lubrication of the human ankle joint in walking with the synovial fluid fltrated by the cartilage with the surface zone worn out: steady pure sliding motion", Journal of Biomechanics, 32, 1999, pp. 1059-1069.

[8] Hlavacek, M."Squeeze-film lubrication of the human ankle joint with synovial fluid filtrated by articular cartilage with the superficial zone worn out". J. Biomech. 33, 1415-1422 (2000).

[9] Ruggiero, A, Gomez E., D. Amato R., "Approximate analytical model for the squeeze-film lubrication of the human ankle joint with synovial fluid filtrated by articular cartilage" Tribology Letters 2010; 41 (2):337–43.

[10] Miroslav H., "Lubrication of the Human Ankle Joint in Running", International Review of Mechanical Engineering, 37, 2009, pp. 619- 626.

[11] Alessandro R., Emilio G., Roberto D. "Approximate analytical model for the squeeze-film lubrication of the human ankle joint with synovial fluid filtrated by articular cartilage", Tribology Letters,41(2), 2010,pp. 337–343.

[12] Albert E. Yousif, Ali Amer Al-allaq, "The hydrodynamic squeeze film lubrication of the ankle joint", International Journal of Mechanical Engineering and Applications 2013; 1(2): 34-42.

[13] Amato, R. D, R. Calvo , E. Gomez, "Sensitivity study of the morphometric fitting on the pressure field inside ankle joints", Case Studies in Mechanical Systems and Signal Processing 1 (2015) 8–14,.

[14] Dowson, D. (1980). "Lubrication of joints. A. Natural joints. An introduction to the biomechanics of joints and joint replacements", Edited by D. Dowson and V. Wright, Mechanical Engineering Publications Limited, Suffolk.

[15] Walicki E, "Mathematical modeling of some biological bearings". Smart Materials and Structures 2000; 9: 280–3.

[16] Bujurke NM, Bhavi SG, Naduvinamani NB. "The effect of couple stresses in squeeze film poroelastic bearings with special reference to synovial joints". IMA Journal of Mathematics Applied in Medicine and Biology 1990; 7:231–43.

[17] Eringen A. C., "Simple Microfluids", International Journal of Engineering Science, 1964, vol. 2, pp. 205-217.

[18] Alessandro R., Emilio G., Roberto D., "Approximate closed-form solution of the synovial fluid film force in the human ankle joint with non-Newtonian lubricant", Tribology International, 57, 2013,pp. 156–161.

[19] Bujurke N. M., Ramesh B. Kudenatti, "An analysis of rough poroelastic bearings with reference to lubrication mechanism of synovial joints", Applied Mathematics and Computation 178, 2006, pp. 309-320.

[20] Naduvinamani N. B., Hiremath P. S., Syeda Tasneem Fathima., "On the squeeze film lubrication of long porous journal bearings with couple stress fluids". Industrial Lubrication and Tribology, vol. 57, 2005, pp. 12-20.

[21] Lin J. R., "Squeeze film characteristics of long partial journal bearings lubricated with couple stress fluids", Tribology International, Vol. 30, 1997, pp. 53-8.

[22] Sinha P., Singh C., Prasad K. R., "Lubrication of Human Joints A Microcontinuum Approach", Wear, 80, 1982, pp. 159-181.

[23] Mokhiamer U. M., Crosby W. A., El – Gamal H. A., "A study of a journal bearing lubricated by fluid with couple stress considering the elasticity of the liner", Wear, 224, 1999, pp. 194 – 201.

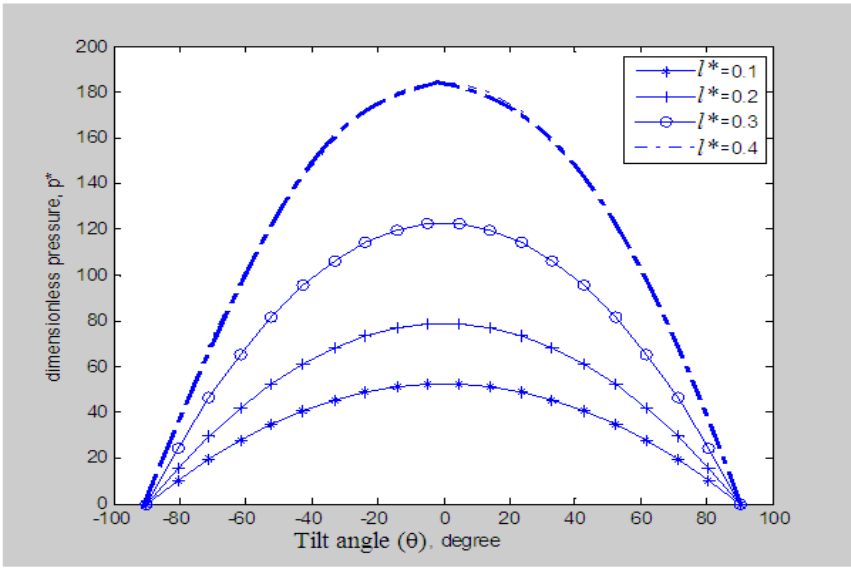

Fig.5: Dimensionless pressure (p*) versus tilt angle (θ) for different dimensionless couple stress length parameters (l*) at (Ø=10^{-8} m^2), (ε = 0. 2), (β=0.3), (h*=0.3), (l*=0.3).

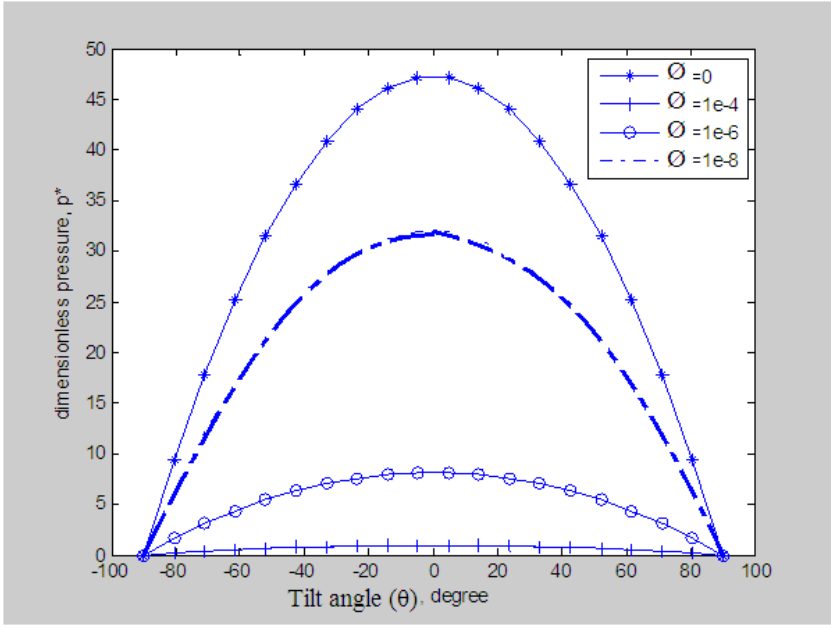

Fig.6: Dimensionless pressure (p*) versus tilt angle (θ) for different permeability value of the cartilage matrix permeability (Ø) at (ε = 0. 2), (β=0.3), (h*=0.3), (l*=0.3).

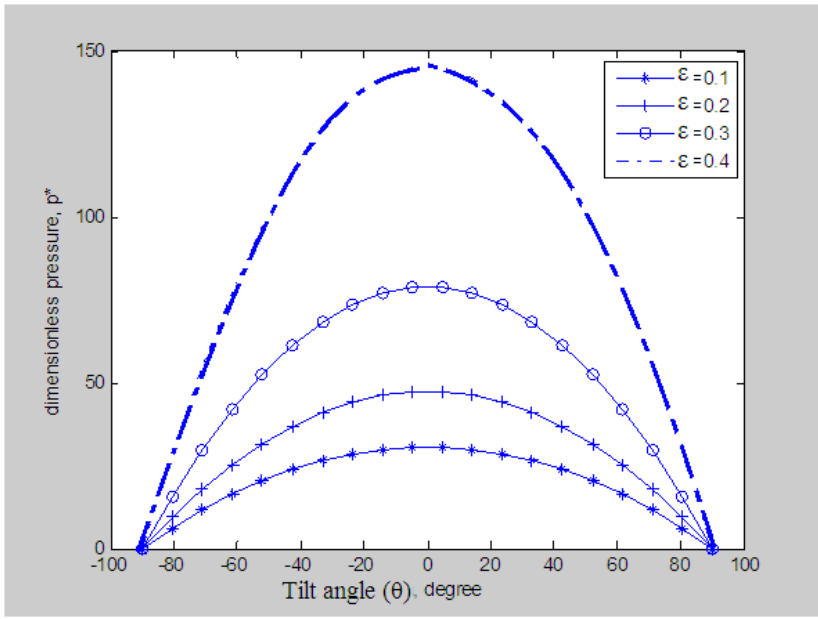

Fig.7: Variation of dimensionless pressure (p*) with tilt angle (θ) for different dimensionless eccentricity ratio (ε*), at (Ø=10^{-8} m^2), (β=0.3), (h*=0.3), (l*=0.3).

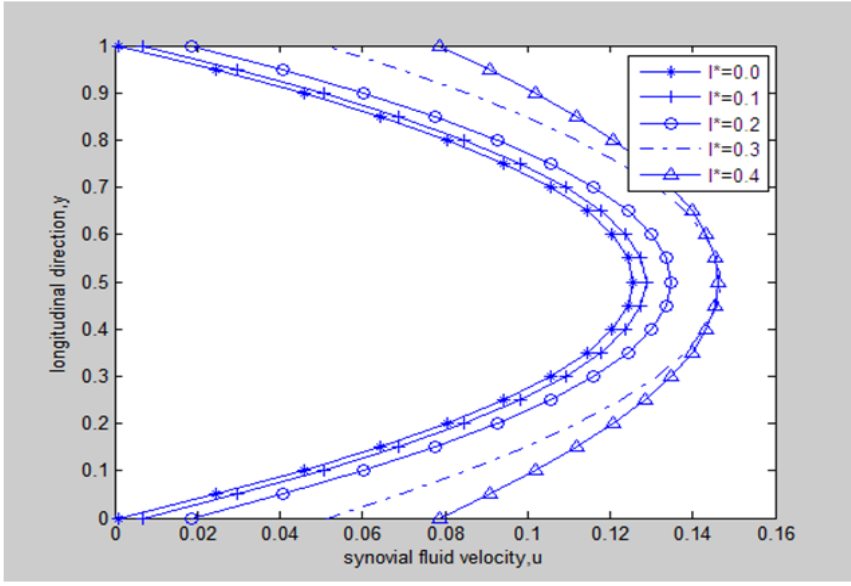

Fig.8. Effect of dimensionless couple stress length parameter (l*) on the synovial fluid film axial velocity (u) at (Ø=10^{-8} m^2), (ε = 0. 2), (β=0.3), (h*=0.3).

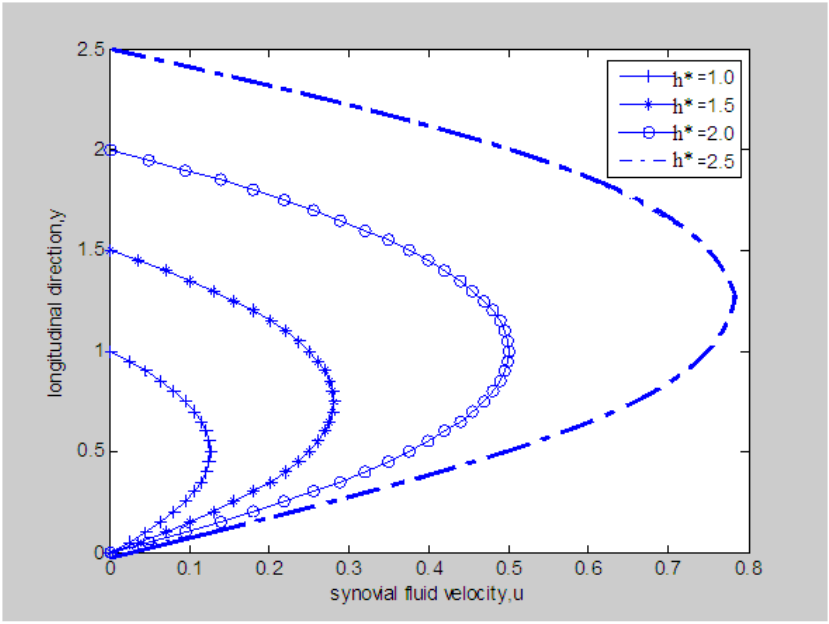

Fig.9. Effect of synovial film thickness (h 10^{-4}) on the synovial fluid film axial velocity (u) at (Ø=10^{-8} m^2), (ε = 0. 2), (β=0.3), (l*=0.3).

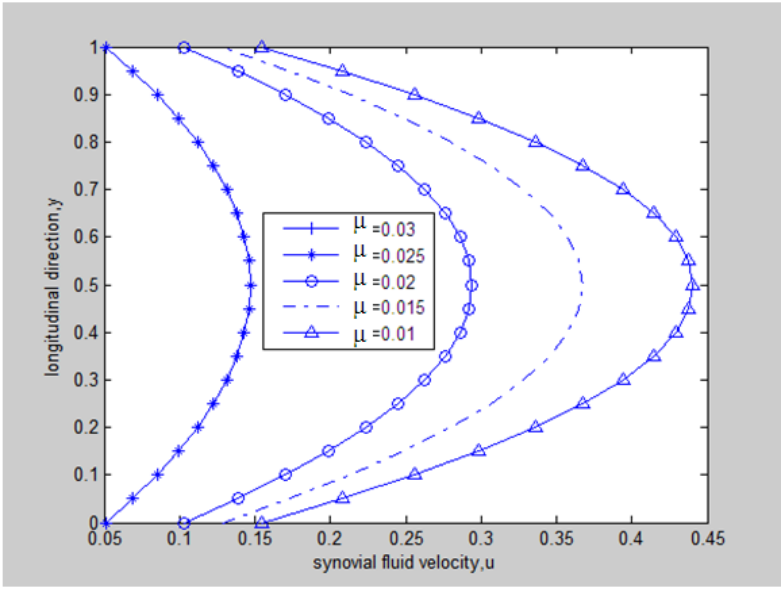

Fig.10. Effect of viscosity of synovial fluid (μ) on the synovial fluid film axial velocity at (Ø=10^{-8} m^2), (ε = 0. 2), (β=0.3), (h*=0.3), (l*=0.3).

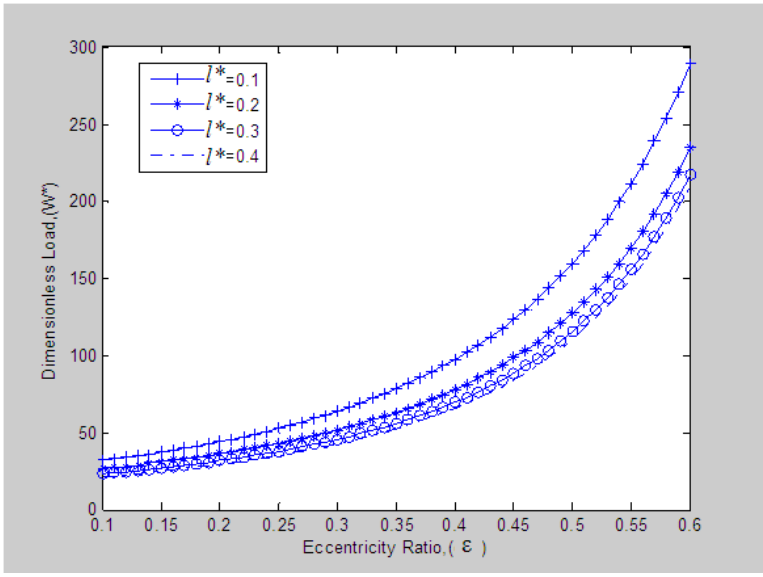

Fig.11. Effect of dimensionless couple stress length parameters (l*) on dimensionless load capacity (W*) at (Ø=10^{-8} m^2), (β=0.3), (h*=0.3).

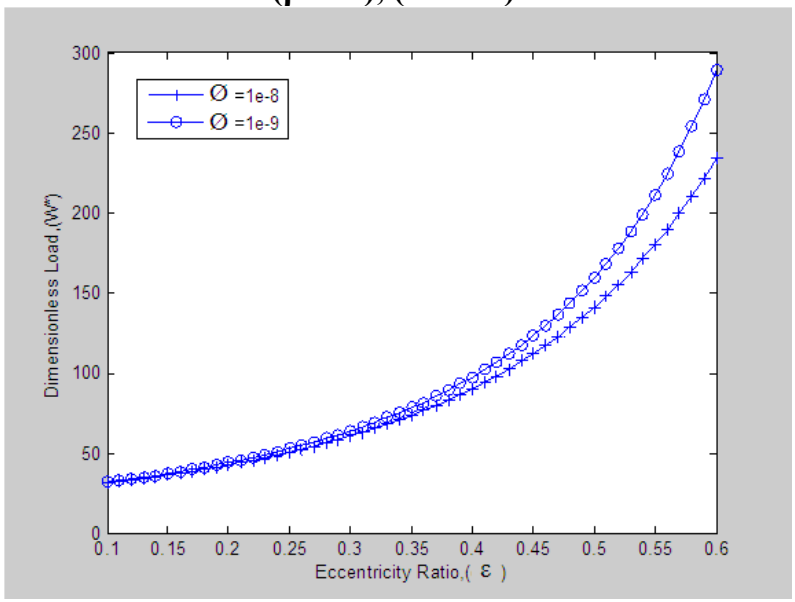

Fig.12: Variation of dimensionless load capacity (W*) with dimensionless eccentricity ratio (ε*) for two permeability value of the cartilage matrix (Ø) at (β=0.3), (h*=0.3), (l*=0.3).

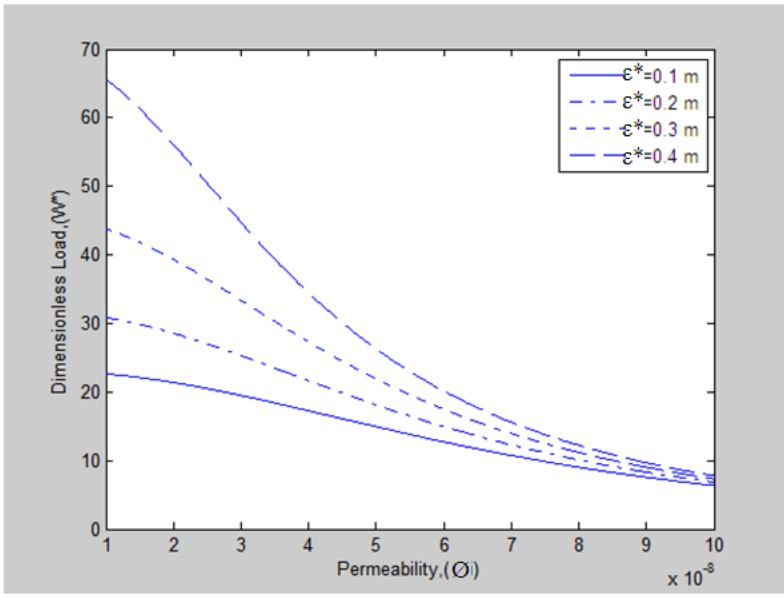

Fig.13: Variation of dimensionless load capacity (W*) with permeability value of the cartilage matrix (Ø) for different value dimensionless eccentricity (ε*) at (β=0.3), (h*=0.3), (l*=0.3).

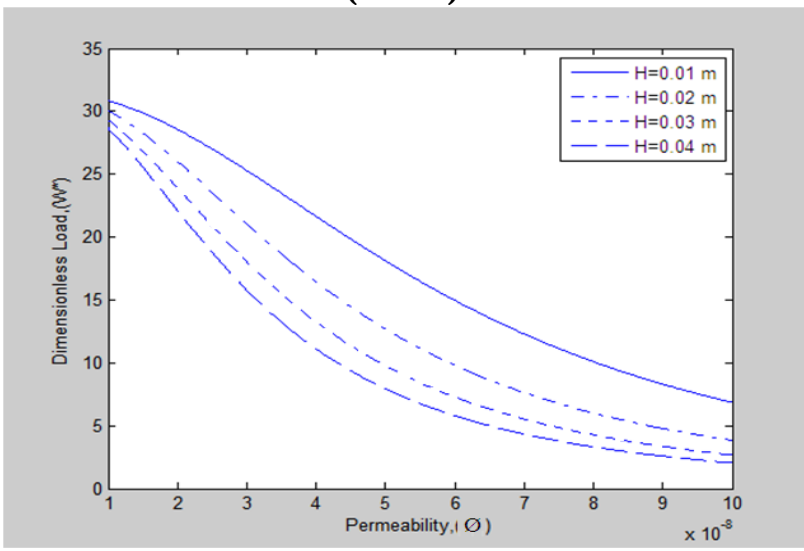

Fig.14: Variation of dimensionless load capacity (W*) with permeability value of the cartilage matrix (Ø) for different value porous layer thickness (H) at (ε = 0. 2), (β=0.3), (h*=0.3), (l*=0.3).

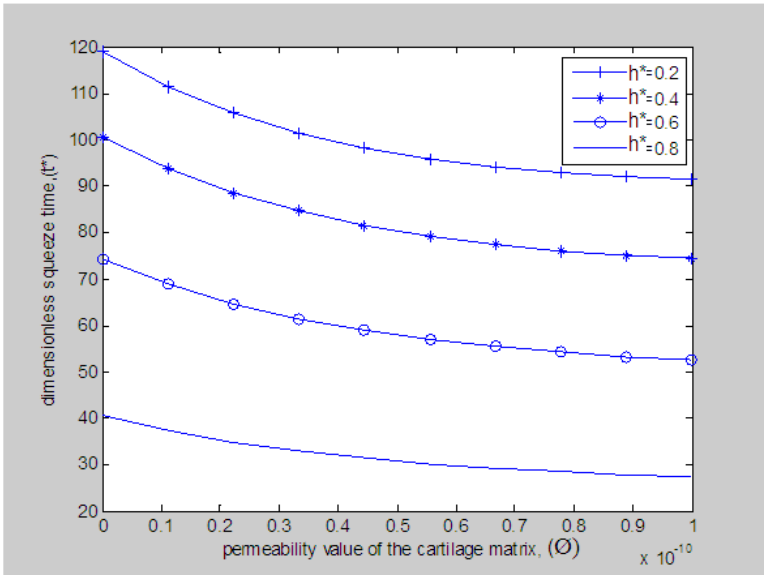

Fig.15. Effect of dimensionless synovial film thickness (h*) on dimensionless response time (t*) (ε = 0. 2), (β=0.3), (l*=0.3).

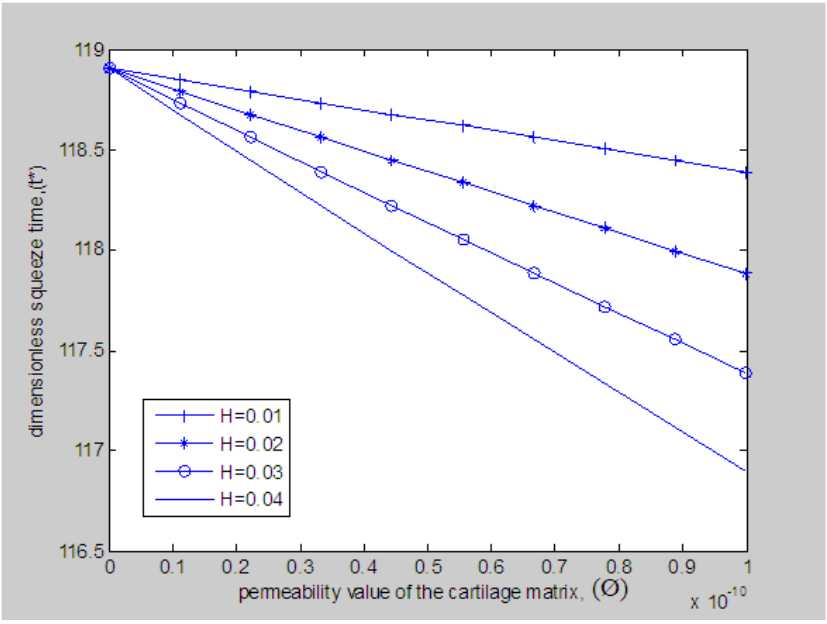

Fig.16. Effect of porous layer thickness (H, mm) on dimensionless response time (t*) at (ε = 0. 2), (β=0.3), (h*=0.3), (l*=0.3).

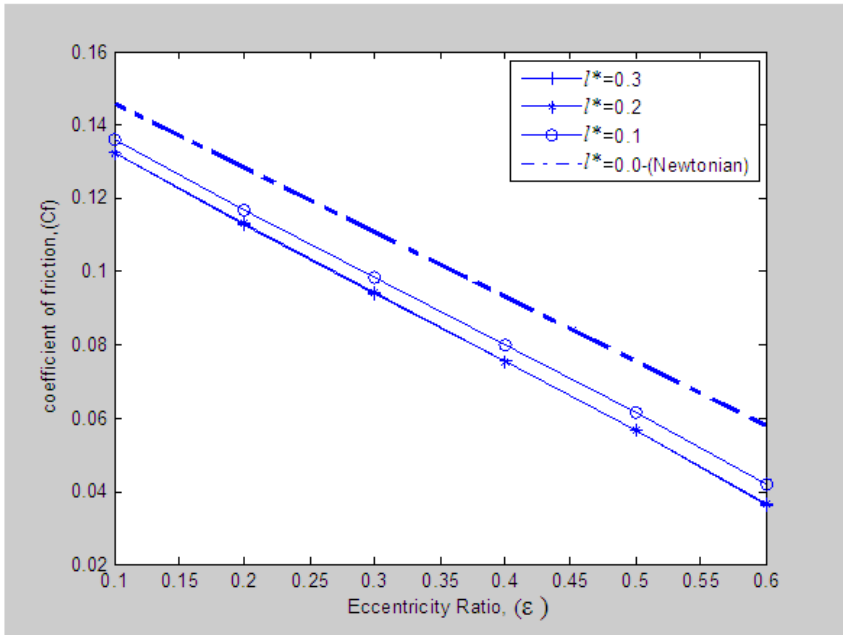

Fig.17. Effect of dimensionless couple stress length parameter (l*) on coefficient of friction (μ) at (Ø=10^{-8} m^2), (β=0.3), (h*=0.3).

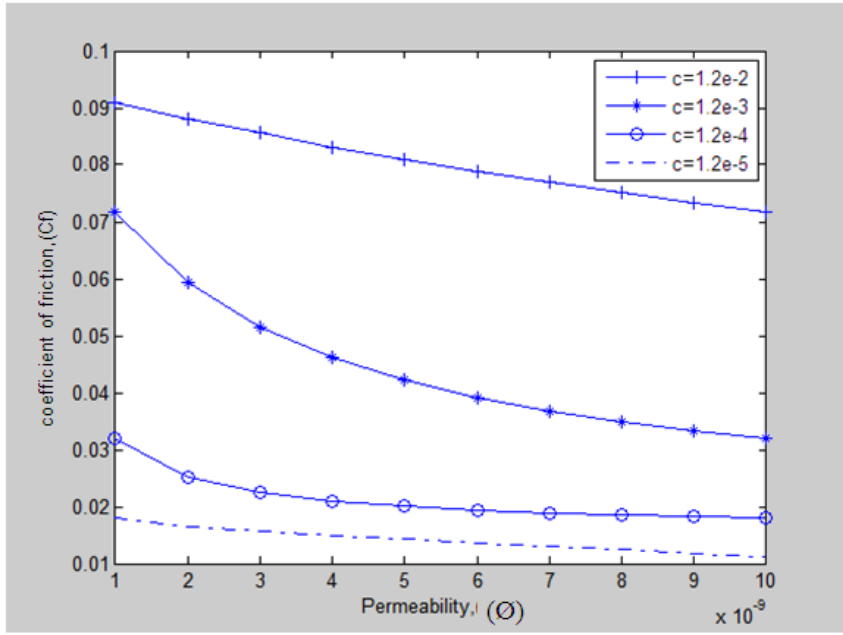

Fig.18. Effect of radial clearance (c) on coefficient of friction (μ) at (ε = 0. 2), (β=0.3), (h*=0.3), (l*=0.3).

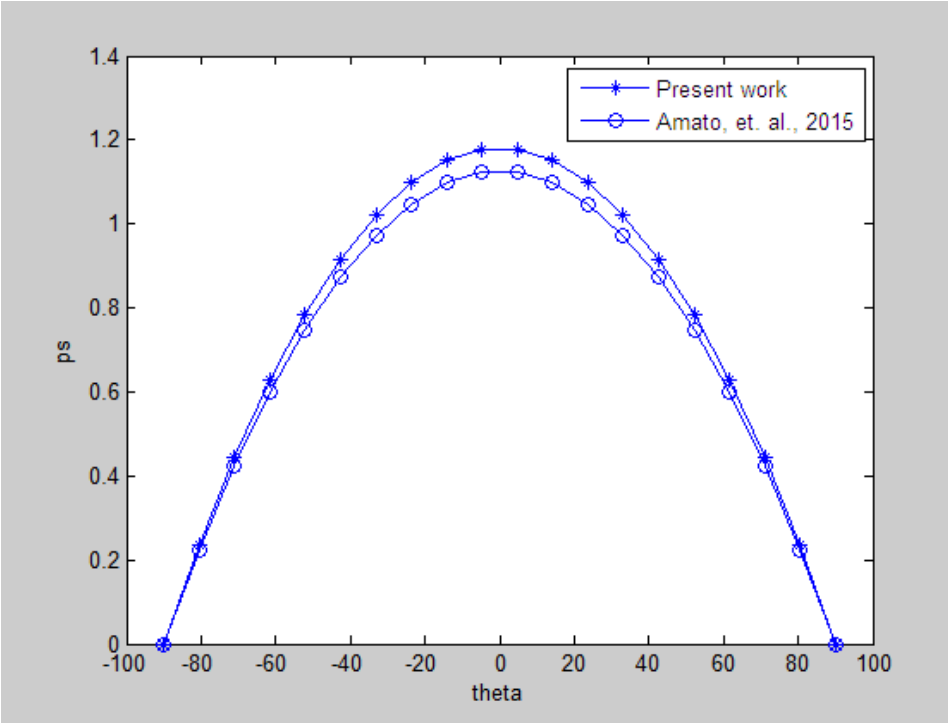

Fig.19. Comparison the present work dimensionless pressure (p*) with tilt angle (θ) with result of (Amato, et. al., 2015) [13] at (ε = 0. 2), (β=0.3), (h*=0.3), (l*=0.3).

دراسة تحليلية للتزييت التنافذي لمفصل الكاحل الزليلي

د. كاظم عودة جحف
kadhum.audaa@yahoo.com
الجامعة التقنية الوسطى - معهد تكنلوجيا- بغداد - قسم المكائن والمعدات
د. صفاء عبد الواحد غضبان
safaaabid@yahoo.com
الجامعة التقنية الوسطى - الكلية التقنية الهندسية الكهربائية
قسم تقنيات القدرة الكهربائية

المستخلص

في البحث الحالي تم نمذجة عملية تزييت مفصل الكاحل للانسان. وتم اعتبار العديد من المتغيرات من مثل متغيرات الشكل الهندسي مثل (اقل سمك للغشاء h, السماحية القطرية c, اللامركزية e) متغيرات عملية التزييت مثل (لزوجة السائل الزليلي μ , خاصية الاجهاد المزدوج η) واخيرا متغيرات شبكة الغضروف مثل (نسبة حجم التركيب الميكروي β , نفاذية الغضروف ϕ , سمك الطبقة المسامية H) وبتحليل تاثيرات هذه المتغيرات على كل من توزيع الضغط المحوري للمنطقة المسامية, سعة التحميل لكل وحدة طول تزييت المفصل ومعامل احتكاك المفصل. وقد بدأ النموذج من نظرية التزييت التنافذي للمفاصل الغضروفية للانسان وباخذ في نظر الاعتبار انتقالية المائع عبر غضروف المفصل باستخدام معادلة رينولدز ومعادلة دارسي المعدلة. وقد اظهرت النتائج ان الضغط المحوري يزداد بزيادة عامل طول الاجهاد المزدوج ومعامل النسبة اللامركزية. ووجد ان سلوك سرعة السائل الزليلي تغيرت من السلوك النيوتيني عند ($l^*=0.0$) الى السلوك الغير نيوتيني مع زيادة عامل طول الاجهاد المزدوج. واخيرا فان معامل الاحتكاك يزداد مع نقصان النسبة اللامركزية وزيادة السماحية القطرية للمفصل.

الكلمات الرئيسية: مفصل الكاحل, التزييت التنافذي, تزييت المفاصل الزليلية